

# Automated Indirect Transport of Biological Cells Using Planar Gripper Formations

Sagar Chowdhury, *Student member, IEEE*, Atul Thakur, *Member, IEEE*, Chenlu Wang, Petr Svec, Wolfgang Losert, and Satyandra K. Gupta, *Member, IEEE*

**Abstract**—Optical tweezers are used for manipulation of micron-sized dielectric beads and cells. Some biological cells are vulnerable to photo damage if subjected to laser based direct manipulation. In such cases, precise manipulation of these cells can be accomplished by using gripper formations made up of glass beads actuated by optical tweezers. Indirect manual manipulation of cells using optically held micro-beads is a time consuming process or sometimes just impossible. This paper reports an approach for automated micromanipulation using gripper formations and an A\* based path planning for collision-free transport of biological cells. The objective of the heuristic planner is to transport the cell in minimum time. Using the designed experiments, we evaluated the performance of different gripper formations in terms of gripper stability, speed of transport, and required laser power.

## I. INTRODUCTION

Manipulation of cells to form assays is the principle task in many biological and biotechnological experiments such as, (1) cell based screening [1], [2], (2) studying environmental effects on cell behavior [3], (3) studying mechanical properties of cell [4], (4) diagnosis for therapy [5], etc. Microfluidics [6], electrophoresis [7], magnetic manipulation [8], AFM [9], Optical Tweezers (OT) [10] are among some of the common techniques used for cell manipulation.

In OT, a highly focused laser beam is used to exert gradient and scattering forces (of the order of few pN) on a particle (size scale ranging from few nanometers to few tens of micrometers) that results in the particle being stably trapped at the focal point. The trapped particle can then be transported by simply moving the laser beam or can be released by switching off the laser. Due to the precise position control and non-contact nature of the manipulation, OT is successfully used in different single cell manipulation operations (e.g., orientating, stretching, and transporting of cells). Holographic Optical Tweezers (HOT) enable generation of multiple traps allowing simultaneous manipulation of multiple objects in 3D.

One of the main challenges in OT based manipulation of biological cells is the *photodamage* resulting into impaired functionality or even death of the cell [10]. Laser photodamage can occur due to the creation of reactive chemical species

Sagar Chowdhury and Satyandra K. Gupta are with the Department of Mechanical Engineering and the Institute for Systems Research, University of Maryland, College Park, MD 20742, USA. Atul Thakur and Petr Svec are with the Department of Mechanical Engineering, University of Maryland, College Park, MD 20742, USA. Chenlu Wang is with the Biophysics Program, University of Maryland, College Park, MD 20742, USA. Wolfgang Losert is with the Department of Physics, Institute for Physical Science and Technology, and the Institute for Research in Electronics and Applied Physics, University of Maryland, College Park, MD 20742, USA.

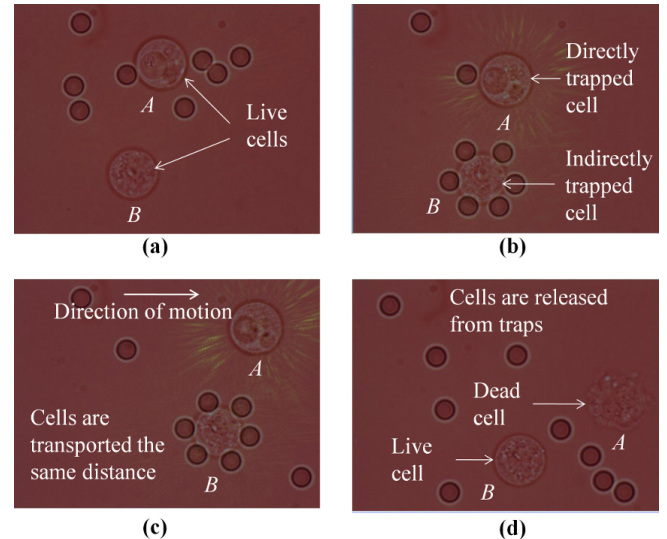


Fig. 1. Direct vs. indirect manipulation using OT: (a) solution of *Dictyostelium discoideum* cell and inert silica microspheres, (b) the cell A is trapped directly, while the cell B is trapped indirectly using a synthesized gripper ( $t = 0$  s), (c) the cells are being transported to their goal locations ( $t = 12$  s), (d) the cells are released at the goal locations; the cell A that was directly trapped is dead, while the indirectly manipulated cell B is still alive ( $t = 15$  s).

[11], local heating [12], two-photon absorption [13], and singlet oxygen through the excitation of photosensitizer [14]. In order to reduce the photodamage, several techniques have been proposed, namely, (1) use of lesser intensity of laser power, (2) use of laser wavelengths ranging from 830nm to 970 nm [14], and (3) use of feedback control. Use of lesser intensity laser may result into weaker traps. Optimization of laser wavelengths require extensive recalibration of OT setup. Feedback control may not cater to huge variety of sensitive cells. We propose indirect manipulation of cells using gripper formations made up of laser trapped dielectric beads [15], [16]. Figure 1 shows the transport operation of two *Dictyostelium discoideum* cells. One is directly held by laser trap while the other is indirectly gripped using six optically trapped silica beads. After 15s both the cells are released from the laser traps. The directly gripped cell has exploded due to the high intensity laser, while the indirectly gripped cell is still alive. This is because, the silica beads allow to indirectly grip the cell and thus prevent direct exposure to laser.

Manipulation of gripper formations manually can be time consuming and in some cases not possible (such as, when

simultaneous movements of multiple cells are required). In this paper we present an approach for automated transport of cells using gripper formations. Main challenges encountered in automated planning for this task include, Brownian motion, dynamical interactions among fluid, beads, and cells, and image processing based measurement uncertainty.

The main contributions of this paper include the following.

- (i.) We present an automated approach for indirect manipulation including rotation and linear displacement of biological cells using planar gripper formations,
- (ii.) We present a global path planner based on A\* algorithm to transport cells using gripper formations along collision-free paths.
- (iii.) We demonstrate experimental results of the developed automated indirect cell transport and path planning.
- (iv.) We present detailed experimental results of the performance evaluation of each gripper formation in terms of formation stability, speed of transport, and the used laser power.

## II. LITERATURE REVIEW

In this section, we will review the literature in the areas of robotic grasping, pushing, and path planning, which are closely related to the problem of automated indirect transport of a cell.

Robotic grasping involves three issues [17], namely, (1) existence of allowable contacts for form closure [19], [20], (2) criteria for form closure [18], (3) algorithms to determine set of allowable contacts for form closure.

Various grasp synthesis algorithms have been proposed [21], [20]. Another stream of research deals with the quality of a grasp by developing different metrics [22]. Chowdhury *et al.* [15] synthesized a gripper configuration for manipulating a cell using HOT in 3D.

Akella and Mason [23] generated open-loop feedback plans to push a polygonal object using a fence. Balorda and Bazd [24] reduced uncertainty in pushing an object rather than using expensive fixtures arrangements to compensate for it. Lynch and Mason [25], [26] generated collision-free paths for stable pushing of heavy objects with multiple pusher objects. Rezzoug and Gorce [27] dynamically controlled the multi-finger pushing operation by considering optimal force distribution and center of mass acceleration correction. Berretty *et al.* [28] developed approach to generate sequence of pushing actions to orient parts in a sensor-less manufacturing setup. Similar approach was used by [29] to orient parts in any arbitrary orientation.

Koenig and Likhachev [32] used heuristic based search with the reuse of past information about the environment for fast replanning in unknown terrains. Ferguson *et al.* [33] modified the same heuristic based search to enable *anytime* capability. Missiuro and Roy [34] in their probabilistic roadmap (PRM) planner made the sampling of the state space biased to specific state space areas by calculating the collision probability for certain sampled states. The Rapidly Exploring Random Tree (RRT) algorithm was modified by representing the extended nodes by a distribution of states

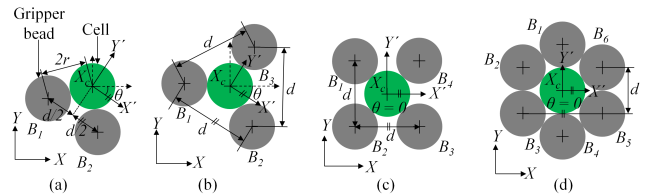


Fig. 2. Gripper formations: (a) Two-bead formation, (b) Three-bead formation, (c) Four-bead formation, (d) Six-bead formation

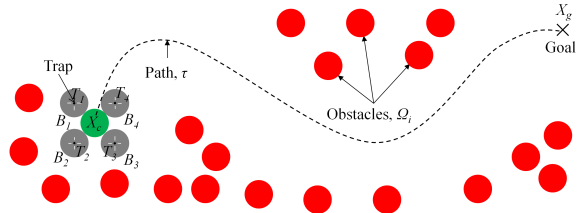


Fig. 3. Problem statement

rather than by a single state [35] for planning under uncertainty. Another extension of RRT to incorporate anytime capability was presented in [36]. The nodes were sampled in [37] according to a suitable probability distribution and thereby an uncertainty roadmap was developed. In optical tweezers based automated particle transport domain, Banerjee *et al.* [30], [31] reported partially ordered Markov decision processes (POMDP) based approach to deal with uncertainties and obstacles. Hu and Sun [38], [39] developed a control architecture for automated transport of biological cells using OT without collision avoidance.

A summary of the literature review and the main issues this paper deals with, are as follows:

- (i.) We can consider 2D relative form closure to grasp the cell since we are transporting the cell in one plane (the focal plane of OT).
- (ii.) Transporting cell by pushing is challenging because of Brownian motion, dynamics of the operating environment, and the measurement noise, which requires a feedback control of formation in order to retain the pusher beads in the formation to push the cell in a desired direction.
- (iii.) In this paper, we use a similar approach developed by [40] where the cost function of the A\* algorithm [41] is modified to find a minimum curved path for automated transport of single yeast cell to a target location using OT. We have modified the cost function of the A\* algorithm to be able to find an optimal resolution and an executable path for a particular gripper formation to minimize the time required for transporting of a cell.

## III. PROBLEM OVERVIEW AND TERMINOLOGY

### A. Terminology

We used the following terminology consistently throughout the paper.

**Gripper Formation** We define a gripper formation as  $G_n = \{X_{B,i} | X_{B,i} \in \mathbb{R}^2, i = 1, 2, \dots, n\}$ , where  $X_{B,i}$

represents the position of a bead  $i$  in  $(X, Y)$  and  $n$  specifies the number of beads in the formation. Figure 2(a) to 2(d) depict the examples of 2, 3, 4, and 6-bead formations  $G_2, G_3, G_4,$  and  $G_6,$  respectively. During the manipulation operation, all the beads  $B_i, i = 1, 2, \dots, n$  are held by their corresponding optical traps  $T_i, i = 1, 2, \dots, n.$

**Gripper Formation Generator** The beads in the gripper formation  $G_n$  are not specified manually. Instead, we designed a generator  $g$  as a function that takes a 4-tuple  $f_n = (X_C, \theta, d, n)$  as an input and produces  $G_n.$  In the tuple,  $X_C$  is the position of the cell  $C$  expressed in  $X$ - $Y,$   $\theta$  is the angular difference between  $X$ - $Y$  and  $X'$ - $Y',$   $d$  is the distance between any two beads in  $F_n$  (assuming a regular configuration), and  $n$  is the number of beads in  $F_n.$  The generator thus allows us to automatically generate the entire gripper configuration using fewer number of parameters which is suitable for optimization [15].

**Gripper Formation State and Maneuvers** We define a continuous 3D state space  $X$  consisting of states  $x \in X$  of the gripper formation  $G_n.$  Each state  $x = [X_c, \theta]^T$  includes the gripper position  $X_C \in \mathbb{R}^2$  (identical to the position of the manipulated cell) and orientation  $\theta$  of the formation in  $(X, Y).$

In addition we define a finite maneuver space  $M(x)$  of the gripper for each state  $x \in X.$  The maneuver  $M(x),$  operating in continuous space  $X$  consists of three atomic maneuvers *rotate,* *translate,* and *retain* that determine a mode of locomotion the gripper formation in the state  $x$  can choose to transport a cell. The *rotate* maneuver represents a function  $m_R(x, \delta\theta) = x',$  where  $x' = [X_c, \theta + \delta\theta]^T,$  that rotates the formation by a constant angle  $\delta\theta.$  The *translate* maneuver represents a function  $m_T(x, \delta d) = x',$  where  $x' = [X_c + \delta d, \theta]^T$  that causes a linear translation for a constant distance  $\delta d = [\delta x, \delta y]^T$  ( $\delta x$  and  $\delta y$  are the translations in  $X$  and  $Y$  directions, respectively). The *retain* maneuver is a special maneuver that enforces the original formation  $G_n$  around the cell if one or more beads get displaced from their required positions. The *retain* maneuver represents a function  $m_{RET}(x) = x$  that retains the formation state to allow the displaced beads to go back to the original formation  $G_n.$  The generator  $g$  takes the desired formation states  $x'$  or  $x$  in  $f_n$  to determine the desired bead positions  $X_{B,i}$  and thereby the next trap positions  $T_i$  as shown in Table I.

**Obstacles** We define a set of obstacles  $\{\Omega_i | \Omega_i = [X_{\Omega,i}, Y_{\Omega,i}] \in \mathbb{R}^2, i = 1, 2, \dots, m\},$  where  $\Omega_i$  represents a position of an obstacle  $i$  in  $(X, Y).$  The set of obstacles includes all the cells and the beads in the workspace besides the beads that are part of  $G_n$  and the cell  $C$  being manipulated in the workspace.

### B. Problem statement

Given a gripper formation  $G_n$  with formation tuple  $f_n$  optically held by traps  $T_i$ s' where  $i = 1, 2, 3, \dots, n$  and randomly moving obstacles  $\Omega_j$ s' where  $j = 1, 2, 3, \dots, N$  find out the following:

- A collision-free global path  $\tau$  to indirectly transport the cell using  $G_n.$

- A complete feedback plan to choose maneuvers for any given gripper formation so that the cell follows the path  $\tau$  or return an *exception* if the current path is no longer valid due to the randomly moving obstacles. In case of *exception,* global path is recomputed.

### C. Assumptions

We made following assumptions:

- We approximate yeast cells and gripper beads as perfect spheres of radius  $r.$  Hence, each obstacle is of radius  $r$  as well.
- We assume that optically trapped beads move with the same velocity as the traps. This is ensured by choosing an operating speed using which the beads can be reliably trapped by the laser traps [42]. Moreover, the planner is assumed to be able to find a collision-free path for the formation. With these assumptions the dynamics of the system can be safely considered to be linear, which will not have any singularity in computing inverse kinematics.

### D. Solution approach

We adopted the following approach (see Fig. 4) to solve the problem:

- We developed four gripper formations (2, 3, 4, and 6-bead) that are able to transport the cell indirectly. We evaluated their performances based on stability, the speed of transport and the required minimum laser power.
- We used Kalman filtering to handle measurement uncertainties.
- We used inverse kinematics to determine the desired trap locations so that the formation can transport the cell along the computed global path.

## IV. PATH PLANNING FOR GRIPPER FORMATION

The planner invokes global path planner at the beginning of the transport or in case of the workspace changes significantly due to the random motion of the freely diffusing beads and cells (see Fig. 4). We use A\* based [41] global planner to find a collision-free path for a gripper formation to transport a cell. We designed a cost function to find a suitable path that minimizes the transport time. In the next two subsections we discuss the state-action space representation of the search space and the cost function.

In order to make search for the path  $\tau$  feasible, we discretize the state space  $X$  into discrete state  $S$  consisting of grid cells with constant size. In this way, the planner can make only constant advancements during the search for  $\tau$  between  $S_i$  and  $S_j.$

### A. State-Action space representation for planning

The discrete state  $S^k$  of a gripper formation is defined as the vector of position  $X_c^k$  of the cell  $C$  and the orientation  $\theta^k$  of the formation at a given time step  $k.$

$$S^k = [X_c^k, \theta^k] \quad (1)$$

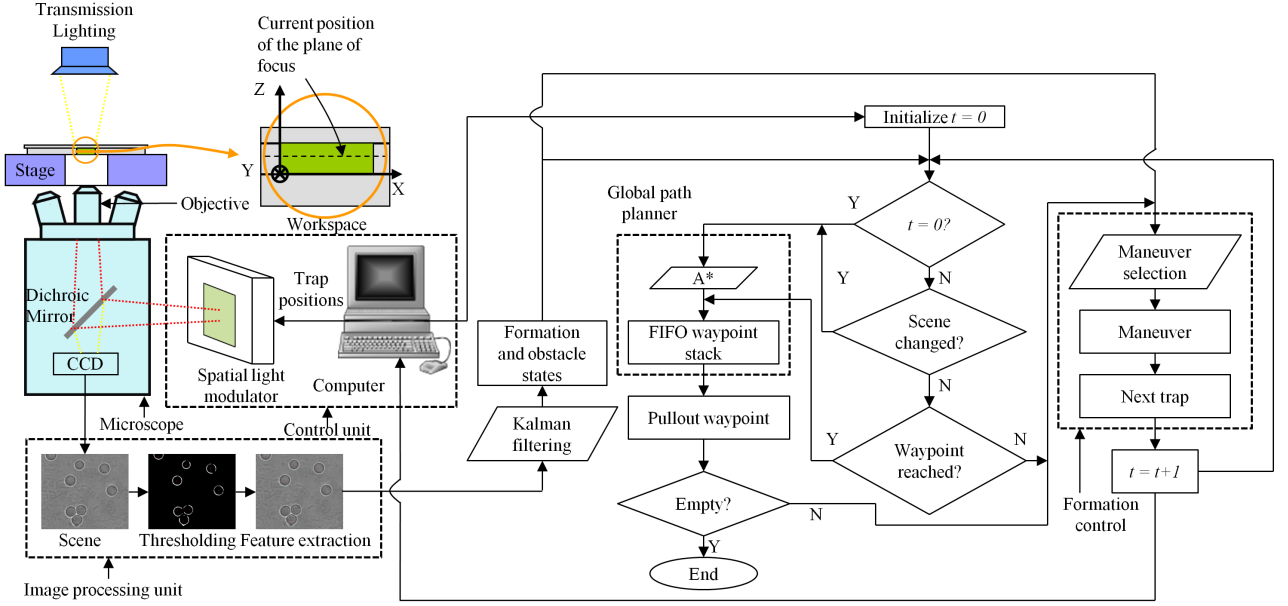


Fig. 4. Solution approach

The state space is represented as a 3D grid with each grid as a state of the formation  $G_n$ . An action is represented as a vector containing a rotation and a linear translation at a given time step  $k$

$$u^k (\delta x^k, \delta y^k, \delta \theta^k) = \begin{bmatrix} \cos \delta \theta^k & -\sin \delta \theta^k & 0 \\ \sin \delta \theta^k & \cos \delta \theta^k & 0 \\ 0 & 0 & 1 \end{bmatrix} \begin{bmatrix} \delta x^k \\ \delta y^k \\ \delta \theta^k \end{bmatrix} \quad (2)$$

Here,  $\delta \theta$  is a constant angular rotation;  $\delta x$  and  $\delta y$  are the linear translations in  $X$  and  $Y$  directions respectively.

When the gripper formation takes an action  $u^k$  at time step  $k$ , it transitions from  $S^k$  to  $S^{k+1}$  using 3

$$S^{k+1} = S^k + u^k \quad (3)$$

### B. Cost function

The planner iteratively expands the nodes of candidate paths in the state-space from initial state  $S_i$  to the goal state  $S_g$  using a cost function

$$f(S) = g(S) + h(S) \quad (4)$$

here,  $f$  is the total cost estimation of a path starting from  $S_i$  to  $S_g$  through state  $S$ ,  $g(S)$  is the optimal cost-to-come from  $S_i$  to  $S$ , and  $h(S)$  is the heuristic cost estimate from  $S$  to  $S_g$ . The formation is transported with a constant speed and thus we use the transport time as the cost estimate. The cost of a newly encountered state  $S'$  is computed as follows:

$$f(S') = g(S) + l(S, u) + h(S') \quad (5)$$

Here,  $l(S, u)$  is the transition cost from states  $S$  to  $S'$ . We use the time of transport for calculating the cost. We use a general cost function  $c(S)$  to calculate transition cost  $l(S, u)$  and heuristic cost  $h(S)$  as shown in 6

$$c(S) = \begin{cases} \frac{L}{v} + \frac{\Delta \theta}{\omega} & \text{if } n < 4, \\ \frac{L}{v} & \text{otherwise,} \end{cases} \quad (6)$$

where  $v$  and  $\omega$  are the constant linear speed and angular speed of the trap ensemble respectively. To calculate  $l(S, u)$ ,  $L$  and  $\Delta \theta$  are taken as the linear and angular displacements resulting from an action  $u$ , while for the calculation of  $h(S)$ , we take the Euclidean distance between the states  $S$  and  $S_g$  as the linear displacement  $L$  and the total angular displacement required to move from  $S$  to  $S_g$  as  $\Delta \theta$ . The beads in a gripper formation should be able to push the gripped cell towards the desired goal location. During the transport of the formation along a given direction, the beads that move along the direction of the cell exert a pushing force (actuator bead) on the cell, whereas other beads maintain the shape of the formation to constrain the motion of the cell. for  $G_4$  and  $G_6$ , there are enough actuator beads to be able to push the cell in any direction. Hence, they don't need to rotate to change the direction of transport while for  $G_2$  and  $G_3$  they need to rotate to be able to orient the actuator beads along the direction of transport. Hence, we don't consider the rotation for  $n \geq 4$  in 6.

### V. FEEDBACK CONTROL FOR GRIPPER FORMATION

We measured the safe operating speed for a particular gripper formation to transport the cell to a given goal location. However, the cell gets gradually drifted from the waypoint due to Brownian motion. Hence, we need a feedback control that will retain gripper beads if the cell deviates beyond a threshold. In each planning interval, the planner executes one of the three maneuvers: *translate*, *rotate*, and *retain* (see Fig. 4). Depending on the next waypoint and the current positions of the gripper beads and the cell, the planner calculates the desired positions of the beads using inverse kinematics. The positions of the gripper beads in terms of the formation tuple are shown in Table I. Once the required positions of the traps are known, the planner can decide

TABLE I

RULES USED BY FORMATION GENERATOR  $g$  TO DETERMINE THE POSITIONS OF BEADS INSIDE THE GRIPPER

Formation type	Bead positions
$G_2$	$X_{B,1} = X_c - D_1 - D_2$ $X_{B,2} = X_c - D_1 + D_2$
$G_3$	$X_{B,1} = X_c - D_1 - D_2$ $X_{B,2} = X_c - D_1 + D_2$ $X_{B,3} = X_c - D_1 + D_3$
$G_4$	$X_{B,i} = X_c + d[\cos(\pi/4 + i\pi/2), \sin(\pi/4 + i\pi/2)]^T$
$G_6$	$X_{B,j} = X_c + d[\cos(\pi/6 + j\pi/3), \sin(\pi/6 + j\pi/3)]^T$
$D_1 = \sqrt{4r^2 - d^2}/4[\cos\theta, \sin\theta]^T$ , $D_2 = d/2[\sin\theta, -\cos\theta]^T$ , $D_3 = \sqrt{3}d/2[\sin\theta, -\cos\theta]^T$ , $i = 1, 2, 3, 4$ ; $j = 1, 2, 3, 4, 5, 6$	

which maneuver to execute. For  $G_4$  and  $G_6$ , the gripper beads need not rotate in order to reach a particular waypoint. Hence, they need only two maneuvers to follow a path. In each planning time interval the next trap positions are selected using the following algorithm: **Formation control algorithm:**

**Input:** Finite nonempty maneuver library, formation tuple  $f_n$ , waypoint library  $W$ , threshold bead deviation  $l_{th}$ , threshold waypoint deviation  $w_{th}$  execution counter  $t$  (see fig. 4).

**Output:** The next positions of the traps  $\{T_i\}_{i=1}^n$ .

**Steps:**

- (i.) If  $t = 0$ , select the first waypoint  $W_p$  from waypoint library  $W$  where  $p = 1$ .
- (ii.) If  $\|X_c - W_p\| \leq w_{th}$ , set  $p = p + 1$ .
- (iii.) Measure the positions of beads  $Z_{B,i} | Z_{B,i} \in \mathbb{R}^n, i = 1, 2, \dots, n$ . If  $\|X_c^{t-1} - Z_{B,i}\| \leq l_{th}$  go to step v.
- (iv.) Select the *retain* maneuver. Use formation generator  $g$  to calculate  $X_{B,i}$ 's based on formation state  $x$  (Table I). For  $\forall T_i \in T : T_i = X_{B,i}$ , return  $T$ .
- (v.) Based on waypoint  $W_p$  and formation state  $x$ , calculate the desired action  $u$ . If the action requires both *rotate* and *translate* maneuvers, first select the *rotate* maneuver. Calculate the desired formation state  $x$  and the corresponding  $\{X_{B,i}\}_{i=1}^n$  using Table I. For  $\forall T_i \in T : T_i = X_{B,i}$ , return  $T$ .

## VI. RESULTS AND DISCUSSIONS

We demonstrate the effectiveness of the planner using a BioRyx 200 (Arryx, Inc., Chicago, IL) holographic laser tweezer (see Fig. 4). The BioRyx 200 consists of a Nikon Eclipse TE 200 inverted microscope, a Spectra-Physics Nd-YAG laser (emitting green light of wavelength 532 nm), a spatial light modulator (SLM), and proprietary phase mask generation software running on a desktop PC. A Nikon Plan Apo 60x/1.4 NA, DIC H oil-immersion objective is used for magnification. The update rate of the SLM is 15 Hz, and the minimum step size is 150 nm. The feedback control is achieved with a second PC equipped with the uEye camera (IDS, Inc., Cambridge, MA) for imaging the workspace and running the software for executing the planning algorithm. We use 5.0  $\mu\text{m}$  diameter silica beads (density of 2000

TABLE II

PERFORMANCE OF THE DESIGNED GRIPPERS

Transport speed ( $\mu\text{m/s}$ )	Min. laser power (watt)			
	$G_2$	$G_3$	$G_4$	$G_6$
7	0.2	0.4	0.6	1.0
8.5	0.3	0.5	0.8	1.5
10	0.5	0.8	1.0	2.0

$\text{kg/m}^3$  and refractive index of 1.46, purchased from Bangs Laboratories, Inc., Fishers, IN) as the gripper beads. We use the same bead as the gripped object to be automatically transported since they resemble the shape of yeast cell.

Both of the beads in  $G_2$  act as actuators (see Fig. 2(a)). Hence, there is risk that the cell will get deviated from the desired location inside the gripper when moving along a curved path. This formation is suitable for transporting the cell along a straight-line path. The formation  $G_3$  (see Fig. 2(b)) has one extra bead which always holds the cell inside the gripper. Both  $G_2$  and  $G_3$  need to stop and then rotate to change the direction of motion. The formation gets destabilized in case of drastic change in the direction of the transport. The formations  $G_4$  and  $G_6$  (see Figs. 2(c) and 2(d)) are much more robust for transporting along a curved path since they don't need to rotate to change the direction of transport. Hence, the required transport time will also be less compared to  $G_2$  and  $G_3$ . However,  $G_4$  sometimes gets destabilized when moving in along its diagonal direction since it can get only one actuator.

A gripper with larger number of beads is more stable but requires higher laser power, which increases the risk of the cell to be exposed to the high intensity laser. Although, by using the gripper beads, the intensity of the laser experienced by the cell is significantly reduced, the laser exposure cannot be fully eliminated. Hence, the lower the laser power, the safer the cell is inside the gripper. We measured the minimum laser power required to transport a cell with a desired speed along a straight line with all gripper formations. The measured parameters shown in Table II indicate that a gripper with fewer number of beads requires lower laser power. However, the stability of the grippers is reduced with the decreased number of beads. Depending on the sensitivity of the cell to the laser and required transport speed, an appropriate gripper can be chosen based on Table II.

Two paths computed by the A\* algorithm that uses the designed cost function (see 6) are shown in Fig. 5. *Path 1* (99 $\mu\text{m}$ ) considers only the linear transport time as cost *path 2* uses both linear and angular transport time. Both the formations  $G_2$  and  $G_3$  take 159 s and 155 s to reach the goal (with a constant linear speed of 1 $\mu\text{m/s}$  and angular speed of 0.25 rad/s) using the two paths, while for both  $G_4$  and  $G_6$  it is 99 s and 108 s, respectively. In order for the  $G_2$  and  $G_3$  to follow the shortest path (*path 1*), they need to reorient frequently, which increases the transport time as well as affect their stability. On the other hand,  $G_4$  and  $G_6$  grippers do not need to reorient in order to change their directions. Hence, they can take shortest path to transport

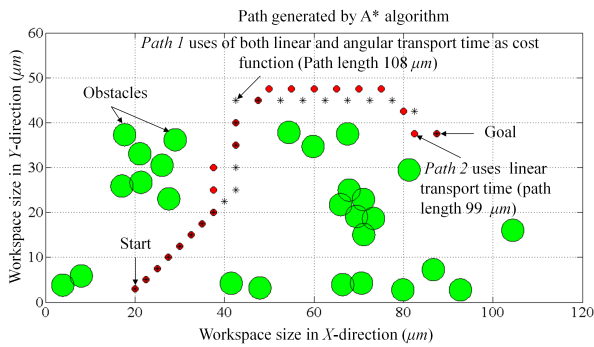


Fig. 5. Path generated using A\* algorithm using the two cost functions

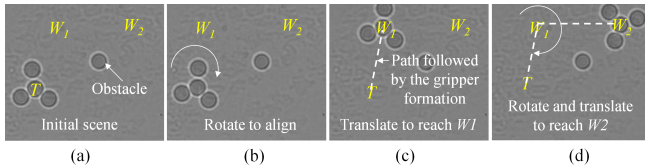


Fig. 6. Indirect transport of a bead using the 3-bead gripper formation: (a) Gripper in the initial state  $T$ , (b) Gripper uses *rotate* maneuver to align itself along the waypoint  $W_1$ , (c) Gripper uses *translate* maneuver to reach the first waypoint  $W_1$ , (d) Gripper uses *rotate* and *translate* maneuvers to reach the final waypoint  $W_2$

the cell.

We show the effectiveness of the formation control (see Section V) by inputting manually selected waypoints to the planner. The waypoints are denoted as  $W$  and an initial location of the gripper is denoted as  $T$ . Each formation successfully follows the waypoints, while transporting the gripped object. Figure 6 shows the selection of different maneuvers by  $G_3$  to follow the waypoints. The formation with two and three beads (see uploaded videos) use the same set of maneuvers to follow similar waypoints. The formation  $G_3$  is more stable than its  $G_2$  counterpart because the extra bead prevents the gripped object from drifting out of the gripper.

Figure 7 shows a target object being transported through two waypoints with  $G_6$  using two maneuvers: *retain* and *translate*. As the gripper bead gets deviated from the desired location, the gripper uses the *retain* maneuver to keep the traps stationary for some time so that the beads can get back to the original formation. The formation  $G_4$  (see uploaded videos) uses same set of maneuvers to transport the gripped

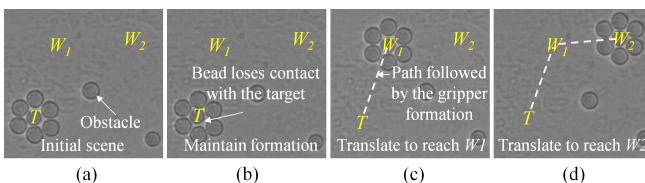


Fig. 7. Indirect transport of a bead using the 6-bead gripper formation: (a) Gripper in the initial state  $T$ , (b) Gripper uses *retain* maneuver to maintain the formation, (c) Gripper uses *translate* maneuver to reach the final waypoint  $W_1$ , (d) Gripper reaches the final waypoint  $W_2$  using only *translate* maneuver

bead.

## VII. CONCLUSIONS AND FUTURE WORK

In this paper, we have designed 2, 3, 4, and 6-bead planar gripper formations, based on the grasping and stable pushing conditions, that are able to reliably transport a gripped object to a desired goal location along a path that minimizes the transport time. We have characterized the gripper formations by measuring the minimum laser power required to transport a gripped cell with a particular speed. We have developed A\* based path planning approach to automatically transport the gripper formations. We have designed a cost function for the developed planner to be able to find executable paths with the least transport time of the gripper formations. Finally, we used a feedback control for the trap positions in order to follow the waypoints without falling apart. We used three types of maneuvers depending on the state of the formation to transport the cell in the desired direction.

In future, we will consider the dynamical interactions between the cell and gripper beads to develop a model predictive control for robust transport of cells. The gripper formations reported in this paper are tested only for transporting spherical cells. In general, cells can be of an arbitrary shape. We will synthesize gripper formations to transport cells of irregular shapes using [15]. It will require rigorous modeling of the cells, beads, and their interactions during the transport.

## ACKNOWLEDGMENT

This research has been supported by NSF grants CMMI-0835572 and CPS-0931508. Opinions expressed are those of the authors and do not necessarily reflect opinions of the sponsors.

## REFERENCES

- [1] X. Wang, Z. Wang, and D. Sun, "Cell sorting with combined optical tweezers and microfluidic chip technologies," in *Control Automation Robotics Vision (ICARCV), 2010 11th International Conference on*, dec. 2010, pp. 201–206.
- [2] Y. Wakamoto, S. Umehara, K. Matsumura, I. Inoue, and K. Yasuda, "Development of non-destructive, non-contact single-cell based differential cell assay using on-chip microcultivation and optical tweezers," *Sensors and Actuators B: Chemical*, vol. 96, no. 3, pp. 693–700, 2003. [Online]. Available: <http://www.sciencedirect.com/science/article/pii/S0925400503005495>
- [3] S. Umehara, Y. Wakamoto, I. Inoue, and K. Yasuda, "On-chip single-cell microcultivation assay for monitoring environmental effects on isolated cells," *Biochemical and Biophysical Research Communications*, vol. 305, no. 3, pp. 534–540, 2003. [Online]. Available: <http://www.sciencedirect.com/science/article/pii/S0006291X03007940>
- [4] P. Bronkhorst, G. Streekstra, J. Grimbergen, E. Nijhof, J. Sixma, and G. Brakenhoff, "A new method to study shape recovery of red blood cells using multiple optical trapping," *Biophysical Journal*, vol. 69, no. 5, pp. 1666–1673, 1995. [Online]. Available: <http://www.sciencedirect.com/science/article/pii/S0006349595800846>
- [5] K. Chen, Y. Qin, F. Zheng, M. Sun, and D. Shi, "Diagnosis of colorectal cancer using raman spectroscopy of laser-trapped single living epithelial cells," *Opt. Lett.*, vol. 31, no. 13, pp. 2015–2017, Jul 2006. [Online]. Available: <http://ol.osa.org/abstract.cfm?URI=ol-31-13-2015>
- [6] S. Chowdhury, P. Svec, C. Wang, K. Seale, J. P. Wiksw, W. Losert, and S. K. Gupta, "Investigation of automated cell manipulation in optical tweezers-assisted microfluidic chamber using simulations," in *Proc. ASME Int. Des. Eng. Tech. Conf. & Comp. Inf. Eng. Conf.*, 2011.

- [7] J. Voldman, "Electrical forces for microscale cell manipulation," *Annual Review of Biomedical Engineering*, vol. 8, no. 1, pp. 425–454, 2006. [Online]. Available: <http://www.annualreviews.org/doi/abs/10.1146/annurev.bioeng.8.061505.095739>
- [8] R. C. Spero, L. Vicci, J. Cribb, D. Bober, V. Swaminathan, E. T. O'Brien, S. L. Rogers, and R. Superfine, "High throughput system for magnetic manipulation of cells, polymers, and biomaterials," *Review of Scientific Instruments*, vol. 79, no. 8, p. 083707, 2008. [Online]. Available: <http://link.aip.org/link/?RSI/79/083707/1>
- [9] R. Roy, W. Chen, L. Goodell, J. Hu, D. Foran, and J. Desai, "Microarray-facilitated mechanical characterization of breast tissue pathology samples using contact-mode atomic force microscopy (afm)," in *Biomedical Robotics and Biomechatronics (BioRob), 2010 3rd IEEE RAS and EMBS International Conference on*, sept. 2010, pp. 710–715.
- [10] A. Ashkin, J. Dziedzic, and T. Yamane, "Optical trapping and manipulation of single cells using infrared-laser beams," *Nature*, vol. 330, no. 6150, pp. 769–771, Dec 1987.
- [11] K. Svoboda and S. Block, "Biological Applications of Optical Forces," *Ann. Rev. Biophys. Biomol. Struct.*, vol. 23, pp. 247–285, Mar 1994.
- [12] Y. Liu, G. Sonek, M. Berns, and B. Tromberg, "Physiological monitoring of optically trapped cells: Assessing the effects of confinement by 1064-nm laser tweezers using microfluorometry," *Biophys. J.*, vol. 71, no. 4, pp. 2158–2167, Oct 1996.
- [13] K. Konig, H. Liang, M. Berns, and B. Tromberg, "Cell-damage by near-in microbeams," *Nature*, vol. 377, no. 6544, pp. 20–21, Sep 1995.
- [14] K. Neuman, E. Chadd, G. Liou, K. Bergman, and S. Block, "Characterization of photodamage to *Escherichia coli* in optical traps," *Biophys. J.*, vol. 77, no. 5, pp. 2856–2863, Nov 1999.
- [15] S. Chowdhury, P. Svec, C. Wang, W. Losert, and S. K. Gupta, "Robust gripper synthesis for indirect manipulation of cells using holographic optical tweezers," in *IEEE Int. Conf. Intell. Robot. Autom.*, 2012, accepted for publication.
- [16] B. Koss, S. Chowdhury, T. Aabo, W. Losert, and S. K. Gupta, "Indirect optical gripping with triplet traps," *J. Opt. Soc. America B*, vol. 28, no. 5, pp. 982–985, Apr. 2011.
- [17] M. T. Mason, *Mechanics of Robotic Manipulation*. The MIT Press, 2001.
- [18] F. Reuleaux, *The Kinematics of Machinery*, A. B. W. Kennedy, Ed. Macmillan and CO., 1876.
- [19] B. Mishra, J. T. Schwartz, and M. Sharir, "On the existence and synthesis of multifinger positive grips," *Algorithmica*, vol. 2, no. 4, pp. 541–558, 1987.
- [20] X. Zhu and H. Ding, "An efficient algorithm for grasp synthesis and fixture layout design in discrete domain," *IEEE Trans. Robot.*, vol. 23, no. 1, pp. 157–163, Feb 2007.
- [21] X. Zhu and J. Wang, "Synthesis of force-closure grasps on 3-d objects based on the q distance," *IEEE Trans. Robot. Automat.*, vol. 19, no. 4, pp. 669–679, Aug 2003.
- [22] M. Roa, R. Suarez, and J. Cornella, "Quality measures for object grasping," *Revista Iberoamericana De Automatica E Informatica Industrial*, vol. 5, no. 1, pp. 66+, 2008.
- [23] S. Akella and M. T. Mason, "Posing polygonal objects in the plane by pushing," in *IEEE International Conference on Robotics and Automation*, vol. 3, May 1992, pp. 2255–2262.
- [24] Z. Balorda and T. Bajd, "Reducing positioning uncertainty of objects by robot pushing," *Robotics and Automation, IEEE Transactions on*, vol. 10, no. 4, pp. 535–541, aug 1994.
- [25] K. Lynch and M. T. Mason, "Stable pushing: Mechanics, controllability, and planning," in *Algorithmic Foundations of Robotics*. Boston, MA: A. K. Peters, 1995, pp. 239–262.
- [26] K. M. Lynch and M. T. Mason, "Stable pushing: Mechanics, controllability, and planning," *Int. J. Robot. Res.*, vol. 15, no. 6, pp. 533–556, 1996.
- [27] N. Rezzoug and P. Gorce, "Dynamic control of pushing operations," *Robotica*, vol. 17, no. 06, pp. 613–620, 1999. [Online]. Available: <http://dx.doi.org/10.1017/S0263574799001782>
- [28] R.-P. Berretty, M. H. Overmars, and A. F. van der Stappen, "Orienting polyhedral parts by pushing," *Comput. Geom. Theory Appl.*, vol. 21, pp. 21–38, Jan. 2002. [Online]. Available: [http://dx.doi.org/10.1016/S0925-7721\(01\)00043-8](http://dx.doi.org/10.1016/S0925-7721(01)00043-8)
- [29] H. Qiao, "Two- and three-dimensional part orientation by sensor-less grasping and pushing actions: Use of the concept of 'attractive region in environment'," *International Journal of Production Research*, vol. 41, no. 14, pp. 3159–3184, 2003. [Online]. Available: <http://www.tandfonline.com/doi/abs/10.1080/0020754031000110268>
- [30] A. G. Banerjee, S. Chowdhury, W. Losert, and S. K. Gupta, "Survey on indirect optical manipulation of cells, nucleic acids, and motor proteins," *J. Biomed. Opt.*, vol. 16, no. 5, May 2011.
- [31] —, "Real-time path planning for coordinated transport of multiple particles using optical tweezers," *IEEE Trans. Autom. Sci. Eng.*, 2011, in review.
- [32] S. Koenig and M. Likhachev, "Fast replanning for navigation in unknown terrain," *IEEE Trans. Robot.*, vol. 21, no. 3, pp. 354–363, Jun. 2005.
- [33] D. Ferguson, M. Likhachev, and A. T. Stentz, "A guide to heuristic-based path planning," in *Proc. Int. Work. Plan. Uncer. Auto. Syst., Int. Conf. Autom. Plan. Sched.*, Jun. 2005.
- [34] P. Missiuro and N. Roy, "Adapting probabilistic roadmaps to handle uncertain maps," in *Proc. IEEE Int. Conf. Robot. Autom.*, May 2006, pp. 1261–1267.
- [35] N. Mechior and R. Simmons, "Particle rrt for path planning with uncertainty," in *Proc. IEEE Int. Conf. Robot. Autom.*, 2007.
- [36] C. Fulgenzi, A. Spalazani, and C. Laugier, "Probabilistic rapidly exploring random trees for autonomous navigation among moving obstacles," in *Work. Safe Navig., IEEE Int. Conf. Robot. Autom.*, 2009.
- [37] L. Guibas, D. Hsu, H. Kurniawati, and E. Rehman, "Bounded uncertainty roadmaps for path planning," in *Proc. Int. Work. Alg. Found. Robot.*, 2008.
- [38] S. Hu and D. Sun, "Automated transportation of single cells using robot-tweezer manipulation system," *J. Lab. Autom.*, vol. 16, no. 4, pp. 263–270, Aug. 2011.
- [39] —, "Automatic transportation of biological cells with a robot-tweezer manipulation system," *The Int. J. Robot. Res.*, Aug. 2011.
- [40] Y. Wu, Y. Tan, D. Sun, and W. Huang, "Force analysis and path planning of the trapped cell in robotic manipulation with optical tweezers," in *Proc. IEEE Int. Conf. Robot. Autom.*, May 2010, pp. 4119–4124.
- [41] P. Hart, N. Nilsson, and B. Raphael, "A formal basis for the heuristic determination of minimum cost paths," *IEEE Trans. Syst. Sci Cybern.*, vol. 4, no. 2, pp. 100–107, Jul. 1968.
- [42] A. G. Banerjee, A. Balijepalli, S. K. Gupta, and T. W. LeBrun, "Generating Simplified Trapping Probability Models From Simulation of Optical Tweezers System," *J. Comput. Inf. Sci. Eng.*, vol. 9, no. 2, Jun. 2009.